The American Journal of Pathology, Vol. 170, No. 4, April 2007
Copyright © American Society for Investigative Pathology
DOI: 10.2353/ajpath.2007.061028

Tumorigenesis and Neoplastic Progression

Perinecrotic Hypoxia Contributes to Ischemia/Reperfusion-Accelerated Outgrowth of Colorectal Micrometastases

Jarmila D.W. van der Bilt,* Marije E. Soeters,* Annique M.M.J. Duyverman,* Maarten W. Nijkamp,* Petronella O. Witteveen,† Paul J. van Diest,‡ Onno Kranenburg,* and Inne H.M. Borel Rinkes*

From the Departments of Surgery, Medical Oncology,† and Pathology,‡ University Medical Center Utrecht, Utrecht, The Netherlands*

Ischemia/reperfusion (I/R) is often inevitable during hepatic surgery and may stimulate the outgrowth of colorectal micrometastases. Postischemic microcirculatory disturbances contribute to I/R damage and may induce prolonged tissue hypoxia and consequent stabilization of hypoxia-inducible factor (HIF)-1α. The aim of this study was to evaluate the contribution of postischemic microcirculatory disturbances, hypoxia, and HIF-1α to I/R-accelerated tumor growth. Partial hepatic I/R attributable to temporary clamping of the left liver lobe induced microcirculatory failure for up to 5 days. This was accompanied by profound and prolonged perinecrotic tissue hypoxia, stabilization of HIF-1α, and massive perinecrotic outgrowth of preestablished micrometastases. Restoration of the microcirculation by treatment with Atrasentan and L-arginine minimized hypoxia and HIF-1α stabilization and reduced the accelerated outgrowth of micrometastases by 50%. Destabilization of HIF-1α by the HSP90 inhibitor 17-DMAG caused an increase in tissue necrosis but reduced I/R-stimulated tumor growth by more than 70%. In conclusion, prevention of postischemic microcirculatory disturbances and perinecrotic hypoxia reduces the accelerated outgrowth of colorectal liver metastases after I/R. This may, at least in part, be attributed to the prevention of HIF-1α stabilization. Prevention of tissue hypoxia or inhibition of HIF-1α may represent attractive approaches to limiting recurrent tumor growth after hepatic surgery. ***(Am J Pathol 2007, 170:1379–1388; DOI: 10.2353/ajpath.2007.061028)***

The liver is the most common site for metastases, developing in more than 50% of colorectal cancer patients. In selected cases, hepatic resection is the only curative option offering 5-year survival rates of 30 to 40%.[1–4] For nonresectable metastases, focal heat-destruction therapies, such as radiofrequency ablation or laser-induced thermotherapy, have emerged as effective strategies to achieve tumor clearance and to potentially increase life expectancy.[5–7] Unfortunately, the majority of patients ultimately develop recurrent disease from previously undetected micrometastases, predominantly in the liver. During liver resection, the blood flow to the liver is temporarily occluded to prevent excessive blood loss.[8–10] During local ablation, vascular clamping is applied to increase destruction volumes.[11,12] However, vascular clamping induces ischemia/reperfusion (I/R) injury to the liver parenchyma and may contribute to postoperative morbidity.[13–15] Moreover, we have recently demonstrated that the outgrowth of pre-established micrometastases was strongly stimulated after I/R in a murine model.[16] The mechanisms that contribute to this phenomenon are unknown.

Microcirculatory disturbances, attributable to an imbalance of vasoconstrictors (eg, endothelin-1) and vasodilators (eg, nitric oxide), play a pivotal role in the manifestation of I/R injury.[17–21] This no-reflow phenomenon has been extensively studied at the microcirculatory level, but measurements have been limited to relatively short-term reperfusion periods (0 to 120 minutes). Prolonged microcirculatory failure beyond 2 hours of reperfusion may lead to sustained hypoxia in the liver, but data to support this are currently lacking. In response to tissue hypoxia, the transcription factor hypoxia-inducible factor (HIF)-1α is stabilized and acts as a cellular survival factor.[22–28] HIF-1α is a strong stimulator of tumor cell proliferation, anaerobic metabolism, migration, and angiogene-

Supported by The Netherlands Organization for Health Research and Development (grant no. 920-03-313).

Accepted for publication January 10, 2007.

Address reprint requests to Prof. Dr. Inne H.M. Borel Rinkes, M.D., Ph.D., Department of Surgery (G04.228), PO Box 85500, 3508 GA Utrecht, The Netherlands. E-mail: i.h.m.borelrinkes@umcutrecht.nl.

sis.[29–33] Thus, hypoxia and consequent stabilization of HIF-1α in tissue areas containing residual micrometastases may lead to enhanced tumor cell growth.

The aim of this study was to assess the role of microcirculatory disturbances and hypoxia on the outgrowth of micrometastases after I/R. Therefore, we investigated whether improvement of the microcirculation by restoring the endothelin-1/nitric oxide balance by means of Atrasentan and L-arginine could reduce tissue hypoxia and thereby prevent the accelerated outgrowth of pre-established micrometastases after I/R. Moreover, we used the geldanamycin analogue 17-DMAG, which has been shown to induce a von Hippel-Lindau-independent degradation of HIF-1α[34,35] and inhibit hypoxia-dependent tumor growth.[36,37] We investigated whether destabilization of HIF-1α by 17-DMAG could reduce I/R-accelerated tumor growth.

Materials and Methods

Animals

All experiments were performed in accordance with the guidelines of the Animal Welfare Committee of the University Medical Centre Utrecht, Utrecht, The Netherlands. Male BALB/c mice (10 to 12 weeks of age) were purchased from Charles River (Sulzfeld, Germany) and housed under standard laboratory conditions.

Drug Characteristics

Atrasentan (ABT-627), a selective endothelin-A receptor antagonist, was kindly provided by Abbott Laboratories (Abbott Park, IL). Atrasentan was dissolved in 4.2% $NaHCO_3$ and injected intravenously as a single bolus (10 mg/kg body weight) before ischemia, followed by continuous oral administration offered in the drinking water (10 mg/kg body weight per day). The nitric oxide donor L-arginine (Sigma-Aldrich, St. Louis, MO) was administered via continuous subcutaneous infusion using Alzet osmotic minipumps (model 2001; Durect Corp., Cupertino, CA) at a dose of 30 μg/kg/minute starting before ischemia. 17-DMAG (Invivogen, San Diego, CA) was dissolved in saline and administered by intraperitoneal injections at a preoperative dose of 15 mg/kg body weight, followed by three postoperative doses of 7.5 mg/kg body weight every 12 hours after ischemia.

Standardized Murine Model of Hepatic I/R

We used an established model of partial hepatic I/R as previously described.[16] In brief, after a midline incision, temporary ischemia was induced by occluding the vascular inflow of the left lateral liver lobe for 45 minutes. Sham-operated mice underwent laparotomy with exposure of the liver but without interruption of hepatic blood flow. Surgical procedures were performed under isoflurane inhalation anesthesia. Body temperature was maintained at 36.5 to 37.0°C. Nontumor-bearing animals were subjected to left lobar I/R and were randomized to receive control vehicle or Atrasentan treatment combined with L-arginine (n = 8 each group). Sham-operated mice served as controls. After 2 hours, 6 hours, 24 hours, and 5 days of reperfusion, the animals were reanesthetized for measurements of the hepatic microcirculation. At each time point, ethylenediaminetetraacetic acid plasma samples were collected via cardiac puncture for measurements of liver enzymes and livers were harvested and processed for pimonidazole and HIF-1α immunohistochemistry.

Liver Metastases Model

Colorectal liver metastases were induced in mice as described.[16,38,39] In brief, routinely cultured C26 colorectal carcinoma cells were injected into the splenic parenchyma (5×10^4 cells/100 μl). After 10 minutes, the spleen was removed to prevent intrasplenic tumor growth. Five days later, animals were subjected to left lobar I/R and randomized into different treatment groups (n = 8 each group). Mice received either continuous administration of Atrasentan and L-arginine or control vehicle. In a second experiment, I/R-treated mice received either 17-DMAG or control vehicle. Sham-operated mice served as controls (n = 8 each group). Morphometric assessment of tumor growth and hepatic necrosis was performed on nonclamped and clamped liver lobes harvested 5 days later.

Intravital Fluorescence Microscopy

The hepatic microcirculation was analyzed by intravital fluorescence microscopy using a Nikon TE-300 inverted microscope (Uvikon, Bunnik, The Netherlands) equipped with a fluorescence filter for fluorescein isothiocyanate (excitation 450 to 490 nm, emission >515 nm).[40] For contrast enhancement, fluorescein isothiocyanate-labeled dextran (molecular weight 446.000, 2% dextran in 0.9% NaCl; 100 μl per 20 g of body weight) was injected intravenously and excited with blue light (450 to 490 nm). The midline incision was reopened, and the left liver lobe was exteriorized and moistened. The mice were placed on an inverted microscopic stage, using a template to minimize tension and respiratory movement. Body temperature was monitored and maintained at 36.5 to 37.0°C during the entire experiment. Ten to 15 fields were randomly selected per animal and recorded for 10 seconds at a ×40 magnification. Images were captured by a charge-coupled device camera (Exwave HAD; Sony, Badhoevedorp, The Netherlands) and relayed to a personal computer for off-line analysis. Sinusoidal perfusion rates were analyzed by two independent observers, blinded to treatment. Sinusoidal perfusion rates were expressed as the percentage of the number of normally perfused sinusoids divided by the total number of sinusoids observed. Perfusion rates of sham-operated animals were set at 100%. Using this method, interobserver and intraobserver variability was less than 5%.

Liver Enzymes

Plasma levels of alanine aminotransferase and aspartate aminotransferase were analyzed using commercially available diagnostic kits (Instruchemie BV, Delfzijl, The Netherlands) ($n = 8$ each group).

Quantification of Hepatocellular Necrosis

The percentage of hepatocellular necrosis was scored on two nonsequential hematoxylin and eosin (H&E)-stained sections using an interactive video overlay system including an automated microscope (Q-Prodit; Leica Microsystems, Rijswijk, The Netherlands) at a magnification of ×40. Using a four-point grid overlay, the ratio of necrotic cells versus healthy hepatocytes plus tumor cells was determined on at least 100 fields per animal ($n = 8$ each group). The percentage of hepatocellular necrosis was expressed as the mean area ratio of all fields.

Pimonidazole and HIF-1α Immunohistochemistry

Liver samples were harvested, fixed in 4% buffered formalin, paraffin-embedded, and sectioned at 5 μm. Tissue sections of clamped and nonclamped liver lobes were H&E-stained for standard histology. The extent and localization of hypoxia were analyzed using the hypoxia marker pimonidazole hydrochloride (Hypoxyprobe-1, 90201; Chemicon International, Temecula, CA) ($n = 4$ each group).[41,42] Under hypoxic conditions, pimonidazole binds to thiol groups in proteins, peptides, and amino acids and therefore serves as a valuable marker for measuring *in vivo* hypoxia at the cellular level. One hour before termination, pimonidazole was injected intravenously at a dose of 60 mg/kg. Pimonidazole adducts were visualized by immunohistochemistry by using fluorescein isothiocyanate-conjugated mouse anti-Hypoxyprobe-1 monoclonal antibody (1:100, TM 90529; Chemicon International), followed by anti-fluorescein isothiocyanate antibody labeled with horseradish peroxidase (1:50; DAKO, Glostrup, Denmark). For HIF-1α detection, a polyclonal rabbit antibody against mouse HIF-1α was used for incubation overnight (1:50, NB 100-449; Novus, Littleton, CO) and goat anti-rabbit PowerVision+ with 2% mouse serum was used as secondary antibody. Before immunolabeling, endogenous peroxidase activity was blocked using a solution of methanol and hydrogen peroxide. Antigen retrieval was performed by boiling sections for 20 minutes in 0.01 mol/L citrate buffer (pH 6.0) for pimonidazole staining and in ethylenediaminetetraacetic acid-buffered solution (pH 9.0) for HIF-1α staining. Reactions were developed using diaminobenzidine/H_2O_2 as a chromogen substrate. Primary-deleted negative controls were treated with the antibody diluent alone and were all free of nonspecific background staining. Immunostaining for HIF-1α was scored on three to four randomly selected fields at a magnification of ×40 by two independent observers, blinded to treatment ($n =$ 6 each group). The nuclear and cytoplasmic staining patterns were scored as the product of the staining intensity (weak, 1+; moderate, 2+; strong, 3+) and the percentage of positive cells (1 to 10% of cells, 1+; 11 to 50% of cells, 2+; >50% of cells, 3+).

Tumor Load

Intrahepatic tumor load was scored as the hepatic replacement area (HRA).[16,38,39] For each liver lobe at least 100 fields were selected on two nonsequential H&E-stained sections using an interactive video overlay system including an automated microscope (Q-Prodit) at a magnification of ×40. Using a four-point grid overlay, the ratio of tumor cells versus normal hepatocytes plus necrotic cells was determined for each field. Tumor load (HRA) was expressed as the mean area ratio of all fields. Observers were blinded to treatment. Finally, HRA ratios between clamped and nonclamped lobes were calculated for each animal to express the proportional increase in HRA in the clamped (left) lobes versus the nonclamped (right plus median) lobes.

Statistical Analysis

Statistical differences between groups were analyzed using the Mann-Whitney *U*-test. Data are expressed as mean ± SEM, unless otherwise stated.

Results

Microcirculatory Failure after I/R Is Associated with Prolonged Perinecrotic Tissue Hypoxia

Intravital fluorescence microscopy revealed normal hepatic microcirculation with >80% regularly perfused sinusoids in sham-operated animals throughout the study period. I/R induced severe sinusoidal perfusion failure, as shown by a 70% relative reduction of perfused sinusoids after 2 hours of reperfusion when compared with sham-operated mice (Figure 1a). Sinusoidal perfusion rates remained low during the 5-day reperfusion period demonstrating a long-term disturbance of the microcirculation. Concurrently, I/R induced severe hepatocellular injury as shown by elevated levels of plasma alanine aminotransferase (Figure 1b) and aspartate aminotransferase (Figure 1c), with a maximum increase at 6 hours of reperfusion followed by normalization after 5 days. Histopathologically, areas of severe hepatocellular damage were seen at 2 and 6 hours after ischemia in all clamped liver lobes, characterized by hemorrhage, eosinophilic hepatocytes, signs of nuclear pyknosis, and loss of cell-cell contact (Figure 2a). After 24 hours, areas of necrosis started to develop, characterized by a massive infiltration of neutrophils. Five days after I/R, necrotic areas were observed in all animals, covering 17 ± 3% of the clamped liver tissue (Figure 1d). As reported previously, these necrotic areas were surrounded by a massive inflammatory infiltrate (Figure 2a).

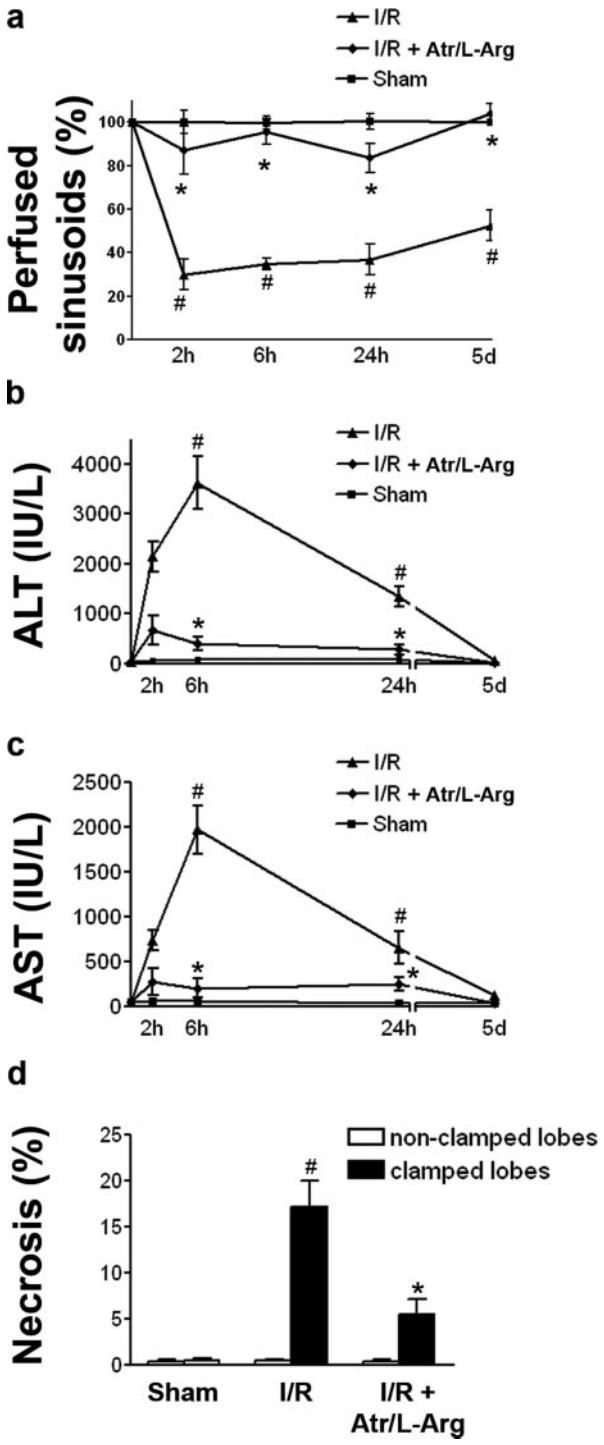

Figure 1. The effect of Atrasentan/L-arginine therapy on I/R-induced microcirculatory disturbances and liver injury. **a:** Hepatic sinusoidal perfusion rates 2 hours, 6 hours, 24 hours, and 5 days after sham operation, I/R, and I/R with Atrasentan/L-arginine therapy ($n = 4$ each group). Hepatocellular damage measured 2 hours, 6 hours, 24 hours, and 5 days after I/R by plasma alanine aminotransferase (ALT) (**b**) and aspartate aminotransferase (AST) (**c**) levels ($n = 8$ each group). **d:** Tissue necrosis, quantified via morphometric analysis of clamped and nonclamped liver lobes at 5 days after clamping ($n = 8$ each group). $^{\#}P < 0.05$ versus sham; $^{*}P < 0.05$ versus I/R.

The extent and localization of hepatic tissue hypoxia after I/R were assessed by pimonidazole immunohistochemistry. In control liver tissue of nonclamped lobes or of sham-operated mice, pimonidazole staining was exclusively observed around central venules, which are known to be characterized by relatively lower oxygen concentrations (Figure 2b).[41] Two hours after I/R, profound diffuse tissue hypoxia was observed throughout the liver parenchyma of the clamped but not of the nonclamped lobes (Figure 2b). During the ensuing 5 days, the liver parenchyma remained remarkably hypoxic. Whereas pimonidazole staining was diffuse after 2 hours of reperfusion, it was selectively localized around areas of hepatocellular necrosis at 5 days after clamping.

Increased Expression of HIF-1α in Hypoxic Tissue Areas

HIF-1α immunohistochemistry was performed on nontumor-bearing tissue sections of livers from sham-operated mice and of clamped and nonclamped liver lobes 2 hours, 6 hours, 24 hours, and 5 days after I/R. In sham-operated mice and in the nonclamped liver lobes, HIF-1α staining was observed around central venules, similar to the pimonidazole staining (Figure 2c).[43] Two hours after I/R, strong cytoplasmic and nuclear HIF-1α staining were observed in hepatocytes throughout the clamped liver lobes (Figure 3, a and b; and Figure 2c). After 6 hours of reperfusion, staining was mainly nuclear and was localized in zones surrounding tissue necrosis (Figure 3, a and b; and Figure 2c). From 24 hours onwards, both cytoplasmic and nuclear HIF-1α staining could still clearly be observed in perinecrotic zones (Figure 3, a and b), which is consistent with the perinecrotic pimonidazole staining (Figure 2c). The nuclear staining at 5 days after clamping was partly attributable to nuclear staining of inflammatory cells surrounding the necrotic tissue areas.

Accelerated Tumor Growth Occurs in Areas of Hypoxia and Increased HIF-1α Expression

I/R resulted in a sixfold to sevenfold increase in micrometastasis outgrowth in occluded liver lobes when compared with nonoccluded liver lobes (Figure 4a). Similar to our earlier observations,[16] accelerated tumor growth was predominantly located around necrotic tissue areas (Figure 4b). We observed a strong association of I/R-stimulated tumor growth with areas of tissue hypoxia and increased parenchymal HIF-1α expression. Strikingly, high levels of HIF-1α were detected in the nuclei of tumor cells at the tumor-necrosis margin, 5 days after clamping (Figure 4c). HIF-1α immunostaining in control tumor tissue in sham-operated mice is rare (Figure 4c).

Attenuation of Microcirculatory Disturbances, Hypoxia, and Hepatocellular Damage by Atrasentan/L-Arginine Is Associated with Reduced Tumor Outgrowth

Treatment with Atrasentan/L-arginine markedly restored the postischemic microcirculation, with a signif-

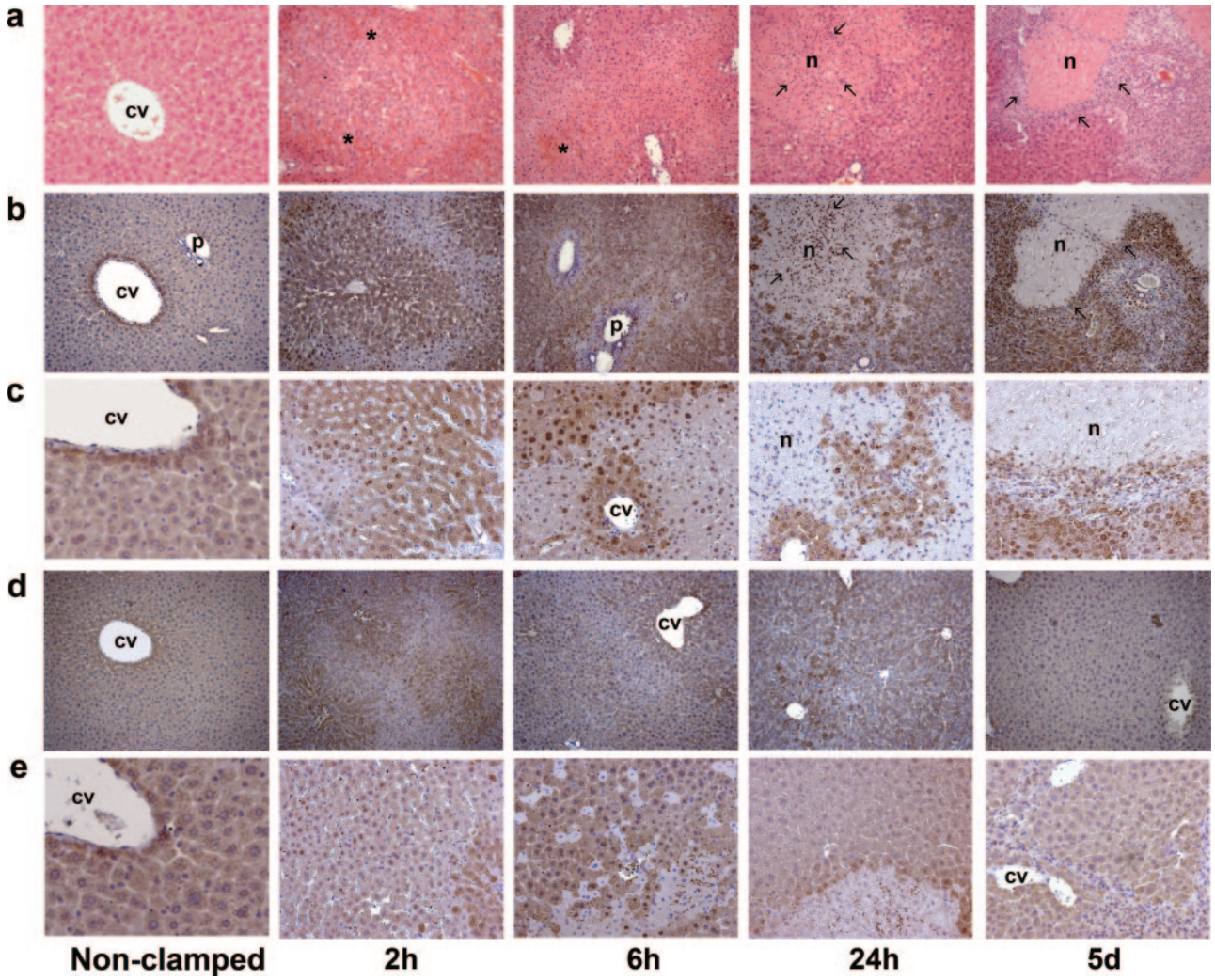

Figure 2. a: H&E-stained tissue sections showing hepatocellular damage characterized by hemorrhage (*), eosinophilic hepatocytes, signs of nuclear pyknosis, and loss of cell-cell contact at 2 and 6 hours of reperfusion, influx of neutrophils (**arrows**) after 24 hours, and areas of necrosis (n) surrounded by an inflammatory infiltrate (**arrows**) 5 days after I/R. **b** and **d:** Tissue hypoxia as shown by pimonidazole immunohistochemistry (brown) 2 hours, 6 hours, 24 hours, and 5 days after hepatic I/R (**b**) and after hepatic I/R with Atrasentan/L-arginine therapy (**d**). **c** and **e:** HIF-1α immunostaining (brown) 2 hours, 6 hours, 24 hours, and 5 days after hepatic I/R (**c**) and after hepatic I/R with Atrasentan/L-arginine therapy (**e**). n, necrosis, cv, central vein, p, portal region. Original magnifications: ×10 (**a**, **b**, **d**); ×20 (**c** and **e**).

icantly higher percentage of perfused sinusoids at all time points when compared with the control vehicle-treated I/R group (Figure 1a). Correspondingly, Atrasentan/L-arginine treatment effectively reduced hepatocellular injury (Figure 1, b and c). In addition, tissue necrosis was reduced by 70% and covered 5 ± 2% of the hepatic tissue (Figure 1d). Pimonidazole immunohistochemistry revealed minimal tissue hypoxia at 2 hours of reperfusion in mice treated with Atrasentan/L-arginine (Figure 2d). At later time points, Atrasentan/L-arginine had completely prevented detectable tissue hypoxia. HIF-1α immunohistochemistry was reminiscent of pimonidazole staining and revealed reduced immunostaining when compared with I/R at all time points (Figure 2e). Despite a distinct cytoplasmic immunostaining at 2 hours of reperfusion, this was not associated with exacerbated nuclear staining (Figure 3, a and b). Next, we investigated whether improvement of the microcirculation and reduction of tissue hypoxia by means of Atrasentan/L-arginine treatment would also reduce tumor growth after I/R. Because Atrasentan and/or L-arginine may influence tumor growth independent of I/R damage, we first evaluated the effect of Atrasentan/L-arginine treatment on tumor growth in sham-operated mice. In these animals, tumor growth was unaffected (data not shown). In mice subjected to I/R, the accelerated outgrowth of micrometastases was inhibited by 50% after Atrasentan/L-arginine treatment (Figure 4a). Interestingly, microscopic evaluation revealed that the few necrotic areas present were surrounded by fields of tumor cells (Figure 4b), which accounted for a residual 50% increase in HRA ratio when compared with sham operation. Similar to the observations in vehicle-treated animals, we found strong nuclear HIF-1α staining in cells at the tumor-necrosis margin (Figure 4c). These

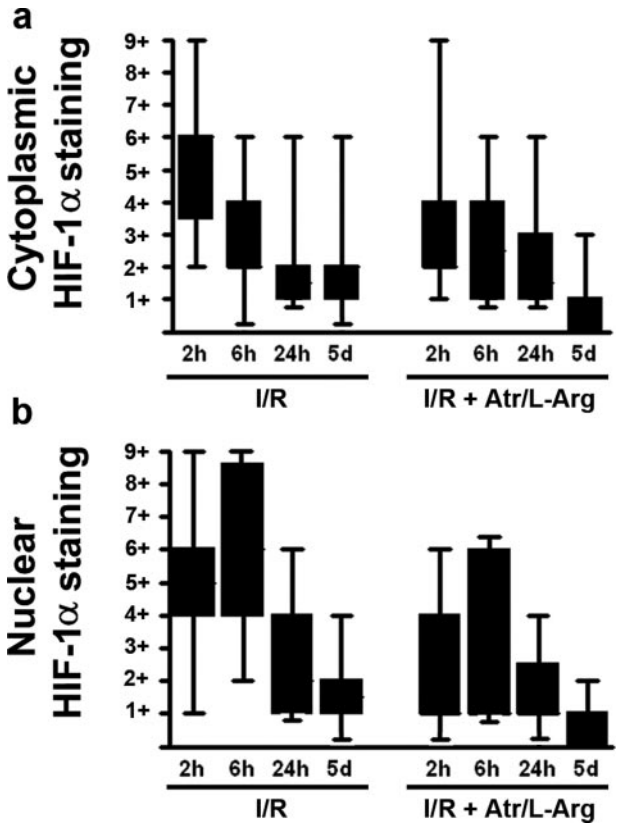

Figure 3. Cytoplasmic (**a**) and nuclear (**b**) HIF-1α immunostaining in clamped liver lobes 2 hours, 6 hours, 24 hours, and 5 days after hepatic I/R and after hepatic I/R with Atrasentan/L-arginine therapy ($n = 6$ each group). Immunostaining was scored as the product of the staining intensity (weak, 1+; moderate, 2+; strong, 3+) and the percentage of positive cells (1 to 10% of cells, 1+; 11 to 50% of cells, 2+; >50% of cells, 3+). Boxes indicate 25 to 75% interval, and lines indicate outer limits.

data strongly suggest that perinecrotic tissue hypoxia and, possibly, the subsequent stabilization of HIF-1α after I/R contribute to the accelerated outgrowth of micrometastases.

Inhibition of I/R-Accelerated Tumor Growth by 17-DMAG

Finally, we used the heat shock protein-90 inhibitor 17-DMAG to promote destabilization of HIF-1α.[34,35] In control vehicle-treated mice, tumor growth was stimulated more than sevenfold after I/R, similar to the first set of experiments (Figure 5, a and b). Again, tumor growth was associated with tissue necrosis (Figure 5, c and d) and positive nuclear HIF-1α immunostaining at the tumor-necrosis margin (Figure 5e). 17-DMAG had no significant inhibitory effect on tumor growth in sham-operated mice (data not shown). Strikingly, 17-DMAG induced a significant reduction in tumor growth in the clamped liver lobes (Figure 5a), without affecting tumor growth in non-clamped liver lobes. This resulted in a 70% decrease in HRA ratio, reflecting a selective inhibitory effect on the perinecrotic stimulation of tumor growth (Figure 5b). Nonetheless, the percentage of necrotic tissue after 17-DMAG had increased from 31 to 56% (Figure 5c), indicating that the treatment had also interfered with the tissue-protecting effect of HIF-1α. Despite this increase in tissue necrosis in the clamped liver lobes, the accelerated perinecrotic tumor growth was not observed (Figure 5d). This is the first time that we observed extensive tissue necrosis without associated tumor growth. Most importantly, microscopic lesions at the necrosis margin

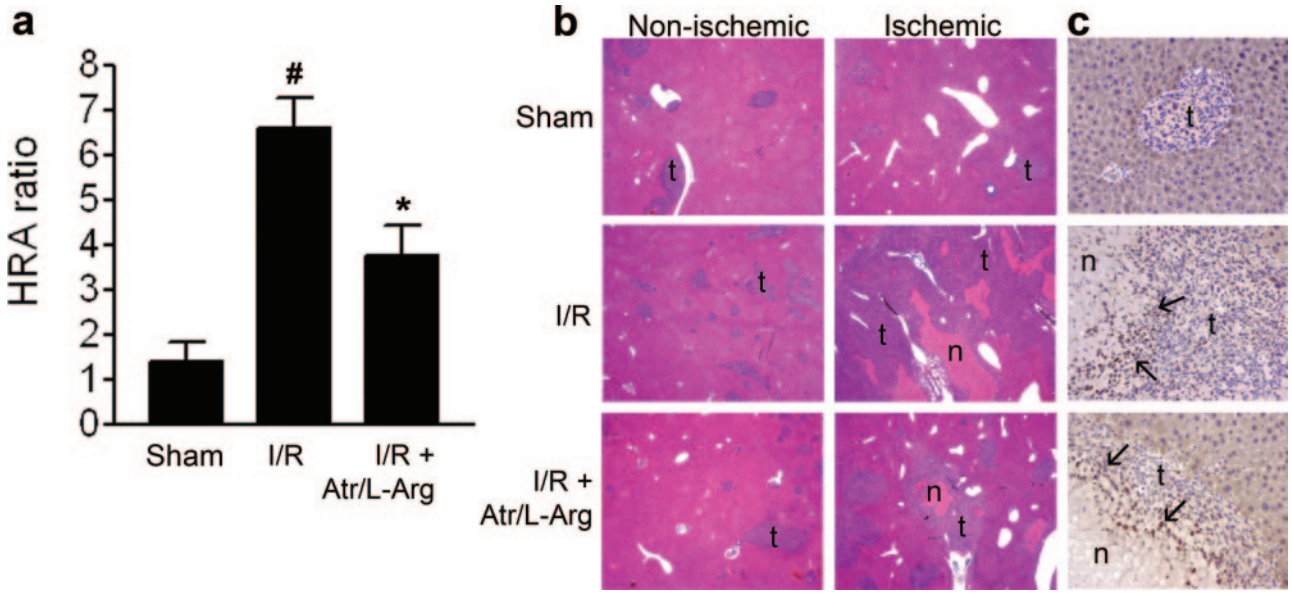

Figure 4. The effect of Atrasentan/L-arginine on the outgrowth of pre-established micrometastases. **a:** Tumor growth expressed as the HRA ratio, the relative increase in the percentage of liver tissue that has been replaced by tumor tissue in ischemic lobes compared with nonischemic lobes ($n = 8$ each group). $^{\#}P <$ 0.05 versus sham; $^{*}P < 0.05$ versus I/R. **b:** Microscopic appearance of I/R-accelerated outgrowth of micrometastases at 5 days after clamping, showing massive tumor (t) growth surrounding necrotic tissue areas (n). **c:** HIF-1α immunostaining in tumor tissue (t) from sham-operated mice and in clamped liver lobes. **Arrows** indicate HIF-1α-positive tumor cells at the tumor-necrosis (n) margin. Original magnifications: ×2 (**b**); ×20 (**c**).

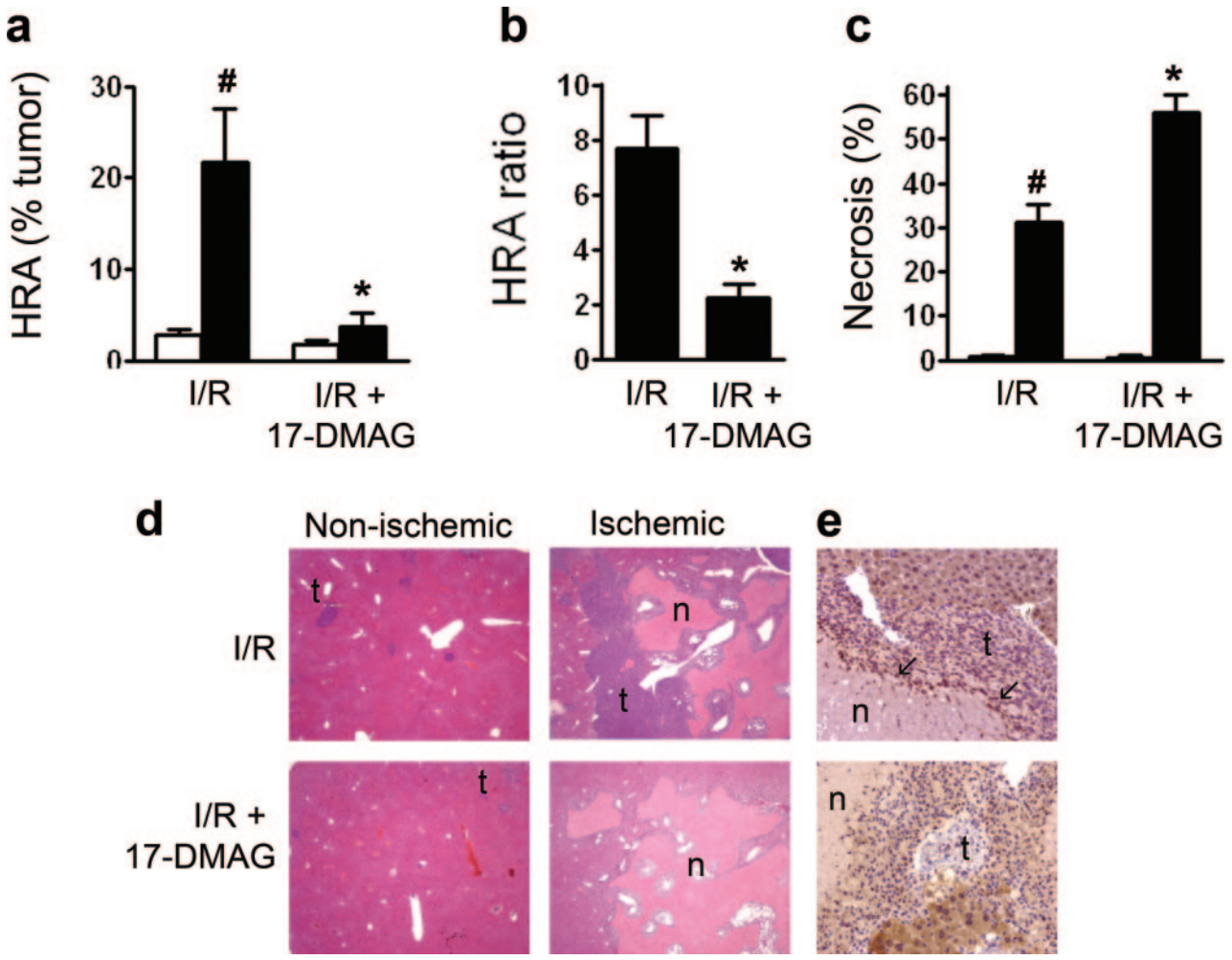

Figure 5. The effect of 17-DMAG on the outgrowth of pre-established micrometastases and tissue necrosis. Tumor growth expressed as the HRA (**a**) and as the HRA ratio (**b**), the relative increase in the percentage of liver tissue that has been replaced by tumor tissue in ischemic lobes compared with nonischemic lobes ($n = 8$ each group). $^{\#}P < 0.05$ versus nonclamped liver lobes; $^{*}P < 0.05$ versus I/R. **c:** Tissue necrosis, quantified via morphometric analysis of clamped and nonclamped liver lobes at 5 days after clamping ($n = 8$ each group). **d:** Microscopic appearance of I/R-accelerated outgrowth of micrometastases at 5 days after clamping, showing massive tumor (t) growth surrounding necrotic tissue areas (n). **e:** HIF-1α immunostaining (brown) in tumor tissue (t) in clamped liver lobes from untreated mice and mice treated with 17-DMAG. **Arrows** indicate HIF-1α-positive tumor cells at the tumor-necrosis (n) margin. Original magnifications: ×2 (**d**); ×20 (**e**).

did not show significant HIF-1α staining, indicating that 17-DMAG indeed prevented HIF-1α stabilization (Figure 5e).

Discussion

The major findings of the work presented here are that 1) the accelerated outgrowth of micrometastases after I/R is associated with long-term microcirculatory disturbances, profound perinecrotic tissue hypoxia and stabilization of HIF-1α; 2) prevention of postischemic microcirculatory disturbances minimizes tissue hypoxia, avoids HIF-1α stabilization, and reduces the accelerated outgrowth of micrometastases; and 3) destabilization of HIF-1α by 17-DMAG reduces I/R-stimulated tumor growth. We conclude that prolonged tissue hypoxia and, possibly, subsequent stabilization of HIF-1α play an important role in the altered behavior of micrometastases in the liver after I/R.

Whereas prolonged periods of hypoxia are deleterious to most cells, tumor cells have adapted to survive under hypoxic conditions.[44] Intratumoral hypoxia has been demonstrated in a number of human cancers, and elevated expression of HIF-1α has been related to tumor aggressiveness.[33,45–49] HIF-1α activates the transcription of several genes that are implicated in cancer progression, including proliferation-promoting cytokines and growth factors; angiogenesis-promoting growth factors; glucose transporters; and serine-, aspartic-, and metalloproteases.[29–33] Thus, prolonged hypoxia as it occurs after I/R may provide a protumorigenic microenvironment through up-regulation of HIF-1α.

Interestingly, pimonidazole and HIF-1α immunostaining were mainly located around necrotic tissue areas. This is consistent with the HIF-1α staining patterns at the necrosis-viable margin of several tumors.[47,50] In the clamped liver lobes, HIF-1α immunoreactivity in hepatocytes was primarily seen after 2 and 6 hours of reperfu-

sion. The strong cytoplasmic staining may be the result of enhanced protein stabilization and accumulation.[43,46,47] It was recently suggested that in the liver, HIF-1α targets to the peroxisome rather than the nucleus after hepatic hypoxia/reoxygenation.[28] We found that HIF-1α staining was sustained up to 5 days, which is consistent with other reports.[51]

We used the geldanamycin analogue 17-DMAG to promote a von Hippel-Lindau-independent degradation of HIF-1α.[34,35] In this study a short-term treatment of 17-DMAG markedly reduced the accelerated outgrowth of micrometastases. Because 17-DMAG inhibits the function of heat shock protein-90, other mechanisms may have co-contributed to the effectiveness of 17-DMAG in reducing postischemic tumor growth. Heat shock proteins are expressed acutely in response to hypoxia and I/R, and they have numerous target genes aimed at promoting cell survival.

Several other mechanisms may have indirectly or directly contributed to I/R-stimulated tumor growth. After I/R, endothelin-1 is increased in the reperfusion period and exerts its vasoconstrictive action via the endothelin-A receptor, contributing to the microcirculatory disturbances after I/R.[52–54] Endothelin-1 may also directly stimulate tumor cell proliferation,[55,56] and its expression correlates with the stabilization of HIF-1α.[57] Finally, the inflammatory response associated with I/R, including the influx of neutrophils and activation of Kupffer cells, may also contribute to the stimulation of tumor growth. Both activated neutrophils and macrophages have been associated with increased metastatic potential, proliferation, and invasion.[58–62] Interestingly, hypoxic macrophages secrete growth factors and angiogenic factors that may favor tumor progression. Furthermore, increased HIF expression has been associated with the presence of tumor-associated macrophages.[63] In addition, the influx of neutrophils contributes to microcirculatory disturbances.[64] Evidently, inflammation and hypoxia mutually influence each other and may co-activate tumor cell proliferation. Our observation that perinecrotic hypoxia was closely associated with the presence of inflammatory cells supports this notion. Thus, tampering the inflammatory response may also minimize hypoxia and thereby reduce tumor growth.

Taken together, although the effects of endogenous (ie, intratumoral) hypoxia on tumor growth have been well documented, this study now shows that exogenous (ie, I/R-induced) hypoxia stimulates tumor growth as well. This may possibly be, at least in part, attributed to the stabilization of HIF-1α. Clinically, this is very relevant because recurrent tumor growth after an apparently complete tumor resection occurs in the majority of patients undergoing liver surgery for colorectal liver metastases. We recently found that severe ischemia as a result from prolonged vascular clamping was associated with a reduced time to develop liver recurrence and a decreased disease-free survival (unpublished data). However, these issues are not only important in case of inevitable clamping of the hepatic blood flow during liver surgery but also during other events that cause I/R injury, such as hemorrhagic shock or sepsis.[65,66] Similar phenomena may occur during surgery-induced tissue hypoxia after wounding, inflammation, and organ manipulation.[42,67–69] Thus, prevention of tissue hypoxia or inhibition of HIF-1α activity may represent attractive approaches to limiting recurrent tumor growth after hepatic surgery. First, therapeutic strategies that restore postischemic microcirculatory flow are potential candidates for reducing I/R-accelerated tumor growth. In the past, several compounds that aim at restoring the endothelin-1/nitric oxide imbalance have been successfully applied to reduce microcirculatory disturbances and liver tissue damage.[18,19,54,70,71] Atrasentan is effective in reducing postischemic microcirculatory disturbances in models of renal,[72] cardiac,[73] and cerebral[74] I/R and we here show that, in combination with the nitric oxide donor L-arginine, it provides maximal improvement of the microcirculation after hepatic I/R. Second, agents that target the HIF-1α pathway, including 17-DMAG, are gaining increased attention as novel anticancer drugs.[75,76] Such compounds may ideally be administered perioperatively to prevent hypoxia-induced tumor growth stimulation. However, HIF-1α is also involved in the physiological response to tissue damage, and thus, their perioperative application may hamper wound and anastomosis healing, which may contribute to increased morbidity. Indeed, we found increased necrosis in clamped liver lobes after treatment with 17-DMAG. Further studies are needed to investigate the effectiveness and safety of such compounds in the postoperative setting.

In conclusion, long-term microcirculatory disturbances, perinecrotic hypoxia, and, possibly, the stabilization of HIF-1α play an important role in the accelerated outgrowth of colorectal liver metastases after I/R. In case of inevitable ischemic damage and hypoxia during hepatic surgery, improving microcirculatory flow or targeting the HIF-1α pathway may decrease the stimulation of microscopic tumor deposits and improve prognosis in colorectal cancer patients.

References

1. Scheele J, Altendorf-Hofmann A: Resection of colorectal liver metastases. Langenbecks Arch Surg 1999, 384:313–327
2. Malafosse R, Penna C, Sa Cunha A, Nordlinger B: Surgical management of hepatic metastases from colorectal malignancies. Ann Oncol 2001, 12:887–894
3. Selzner M, Clavien PA: Resection of hepatic tumors: special emphasis on neoadjuvant and adjuvant therapy. Malignant Liver Tumors: Current and Emerging Therapies. Edited by PA Clavien. Sudbury, Jones and Bartlett Publishers, 2004, pp 153–169
4. Simmonds PC, Primrose JN, Colquitt JL, Garden OJ, Poston GJ, Rees M: Surgical resection of hepatic metastases from colorectal cancer: a systematic review of published studies. Br J Cancer 2006, 94:982–999
5. Heisterkamp J, van Hillegersberg R, Ijzermans JN: Interstitial laser coagulation for hepatic tumours. Br J Surg 1999, 86:293–304
6. Abdalla EK, Vauthey JN, Ellis LM, Ellis V, Pollock R, Broglio KR, Hess K, Curley SA: Recurrence and outcomes following hepatic resection, radiofrequency ablation, and combined resection/ablation for colorectal liver metastases. Ann Surg 2004, 239:818–825
7. McKay A, Dixon E, Taylor M: Current role of radiofrequency ablation for the treatment of colorectal liver metastases. Br J Surg 2006, 93:1192–1201
8. Belghiti J, Marty J, Farges O: Techniques, hemodynamic monitoring,

and indications for vascular clamping during liver resections. J Hepatobiliary Pancreat Surg 1998, 5:69–76
9. Dixon E, Vollmer CM, Bathe OF, Sutherland F: Vascular occlusion to decrease blood loss during hepatic resection. Am J Surg 2005, 190:75–86
10. Smyrniotis V, Farantos C, Kostopanagiotou G, Arkadopoulos N: Vascular control during hepatectomy: review of methods and results. World J Surg 2005, 29:1384–1396
11. Heisterkamp J, van Hillegersberg R, Mulder PG, Sinofsky EL, IJzermans JN: Importance of eliminating portal flow to produce large intrahepatic lesions with interstitial laser coagulation. Br J Surg 1997, 84:1245–1248
12. Patterson EJ, Scudamore CH, Owen DA, Nagy AG, Buczkowski AK: Radiofrequency ablation of porcine liver in vivo: effects of blood flow and treatment time on lesion size. Ann Surg 1998, 227:559–565
13. Carden DL, Granger DN: Pathophysiology of ischaemia-reperfusion injury. J Pathol 2000, 190:255–266
14. Jaeschke H: Molecular mechanisms of hepatic ischemia-reperfusion injury and preconditioning. Am J Physiol 2003, 284:G15–G26
15. Teoh NC, Farrell GC: Hepatic ischemia reperfusion injury: pathogenic mechanisms and basis for hepatoprotection. J Gastroenterol Hepatol 2003, 18:891–902
16. van der Bilt JD, Kranenburg O, Nijkamp MW, Smakman N, Veenendaal LM, te Velde EA, Voest EE, van Diest PJ, Borel Rinkes IHM: Ischemia/reperfusion accelerates the outgrowth of hepatic micrometastases in a highly standardized murine model. Hepatology 2005, 42:165–175
17. Koo A, Komatsu H, Tao G, Inoue M, Guth PH, Kaplowitz N: Contribution of no-reflow phenomenon to hepatic injury after ischemia-reperfusion: evidence for a role for superoxide anion. Hepatology 1992, 15:507–514
18. Pannen BH, Al Adili F, Bauer M, Clemens MG, Geiger KK: Role of endothelins and nitric oxide in hepatic reperfusion injury in the rat. Hepatology 1998, 27:755–764
19. Scommotau S, Uhlmann D, Loffler BM, Breu V, Spiegel HU: Involvement of endothelin/nitric oxide balance in hepatic ischemia/reperfusion injury. Langenbecks Arch Surg 1999, 384:65–70
20. Vollmar B, Glasz J, Leiderer R, Post S, Menger MD: Hepatic microcirculatory perfusion failure is a determinant of liver dysfunction in warm ischemia-reperfusion. Am J Pathol 1994, 145:1421–1431
21. Kondo T, Todoroki T, Hirano T, Schildberg FW, Messmer K: Impact of ischemia-reperfusion injury on dimensional changes of hepatic microvessels. Res Exp Med (Berl) 1998, 198:63–72
22. Martin C, Yu AY, Jiang BH, Davis L, Kimberly D, Hohimer AR, Semenza GL: Cardiac hypertrophy in chronically anemic fetal sheep: increased vascularization is associated with increased myocardial expression of vascular endothelial growth factor and hypoxia-inducible factor 1. Am J Obstet Gynecol 1998, 178:527–534
23. Tacchini L, Radice L, Bernelli-Zazzera A: Differential activation of some transcription factors during rat liver ischemia, reperfusion, and heat shock. J Cell Physiol 1999, 180:255–262
24. Marti HJ, Bernaudin M, Bellail A, Schoch H, Euler M, Petit E, Risau W: Hypoxia induced vascular endothelial growth factor expression precedes neovascularization after cerebral ischemia. Am J Pathol 2000, 156:965–976
25. Pichiule P, Agani F, Chavez JC, Xu K, LaManna JC: HIF-1 alpha and VEGF expression after transient global cerebral ischemia. Adv Exp Med Biol 2003, 530:611–617
26. Chi NC, Karliner JS: Molecular determinants of responses to myocardial ischemia/reperfusion injury: focus on hypoxia-inducible and heat shock factors. Cardiovasc Res 2004, 61:437–447
27. Lee JW, Bae SH, Jeong JW, Kim SH, Kim KW: Hypoxia-inducible factor (HIF-1)alpha: its protein stability and biological functions. Exp Mol Med 2004, 36:1–12
28. Khan Z, Michalopoulos GK, Stolz DB: Peroxisomal localization of hypoxia inducible factors and hypoxia-inducible factor regulatory hydroxylases in primary rat hepatocytes exposed to hypoxia-reoxygenation. Am J Pathol 2006, 169:1251–1269
29. Carmeliet P, Dor Y, Herbert JM, Fukumura D, Brusselmans K, Dewerchin M, Neeman M, Bono F, Abramovitch R, Maxwell P, Koch CJ, Ratcliffe P, Moons L, Jain RK, Collen D, Keshert E: Role of HIF-1alpha in hypoxia-mediated apoptosis, cell proliferation and tumour angiogenesis. Nature 1998, 394:485–490
30. Giatromanolaki A, Harris AL: Tumour hypoxia, hypoxia signaling pathways and hypoxia inducible factor expression in human cancer. Anticancer Res 2001, 21:4317–4324
31. Pugh CW, Ratcliffe PJ: Regulation of angiogenesis by hypoxia: role of the HIF system. Nat Med 2003, 9:677–684
32. Maxwell PH: The HIF pathway in cancer. Semin Cell Dev Biol 2005, 16:523–530
33. Brahimi-Horn C, Pouyssegur J: The role of the hypoxia-inducible factor in tumor metabolism growth and invasion. Bull Cancer 2006, 93:E73–E80
34. Isaacs JS, Jung YJ, Mimnaugh EG, Martinez A, Cuttitta F, Neckers LM: Hsp90 regulates a von Hippel Lindau-independent hypoxia-inducible factor-1 alpha degradative pathway. J Biol Chem 2002, 277:29936–29944
35. Mabjeesh NJ, Post DE, Willard MT, Kaur B, Van Meir EG, Simons JW, Zhong H: Geldanamycin induces degradation of hypoxia-inducible factor 1alpha protein via the proteosome pathway in prostate cancer cells. Cancer Res 2002, 62:2478–2482
36. Zagzag D, Nomura M, Friedlander DR, Blanco CY, Gagner JP, Nomura N, Newcomb EW: Geldanamycin inhibits migration of glioma cells in vitro: a potential role for hypoxia-inducible factor (HIF-1alpha) in glioma cell invasion. J Cell Physiol 2003, 196:394–402
37. Alqawi O, Moghaddas M, Singh G: Effects of geldanamycin on HIF-1alpha mediated angiogenesis and invasion in prostate cancer cells. Prostate Cancer Prostatic Dis 2006, 9:126–135
38. Drixler TA, Borel Rinkes IHM, Ritchie ED, van Vroonhoven TJ, Gebbink MF, Voest EE: Continuous administration of angiostatin inhibits accelerated growth of colorectal liver metastases after partial hepatectomy. Cancer Res 2000, 60:1761–1765
39. te Velde EA, Vogten JM, Gebbink MF, Van Gorp JM, Voest EE, Borel Rinkes IHM: Enhanced antitumour efficacy by combining conventional chemotherapy with angiostatin or endostatin in a liver metastasis model. Br J Surg 2002, 89:1302–1309
40. Vogten JM, Smakman N, Voest EE, Borel Rinkes IHM: Intravital analysis of microcirculation in the regenerating mouse liver. J Surg Res 2003, 113:264–269
41. Arteel GE, Thurman RG, Yates JM, Raleigh JA: Evidence that hypoxia markers detect oxygen gradients in liver: pimonidazole and retrograde perfusion of rat liver. Br J Cancer 1995, 72:889–895
42. Samoszuk MK, Walter J, Mechetner E: Improved immunohistochemical method for detecting hypoxia gradients in mouse tissues and tumors. J Histochem Cytochem 2004, 52:837–839
43. Kietzmann T, Cornesse Y, Brechtel K, Modaressi S, Jungermann K: Perivenous expression of the mRNA of the three hypoxia-inducible factor alpha-subunits, HIF1alpha, HIF2alpha and HIF3alpha, in rat liver. Biochem J 2001, 354:531–537
44. Harris AL: Hypoxia—a key regulatory factor in tumour growth. Nat Rev Cancer 2002, 2:38–47
45. Hockel M, Schlenger K, Aral B, Mitze M, Schaffer U, Vaupel P: Association between tumor hypoxia and malignant progression in advanced cancer of the uterine cervix. Cancer Res 1996, 56:4509–4515
46. Zhong H, De Marzo AM, Laughner E, Lim M, Hilton DA, Zagzag D, Buechler P, Isaacs WB, Semenza GL, Simons JW: Overexpression of hypoxia-inducible factor 1alpha in common human cancers and their metastases. Cancer Res 1999, 59:5830–5835
47. Talks KL, Turley H, Gatter KC, Maxwell PH, Pugh CW, Ratcliffe PJ, Harris AL: The expression and distribution of the hypoxia-inducible factors HIF-1alpha and HIF-2alpha in normal human tissues, cancers, and tumor-associated macrophages. Am J Pathol 2000, 157:411–421
48. Bos R, Zhong H, Hanrahan CF, Mommers EC, Semenza GL, Pinedo HM, Abeloff MD, Simons JW, van Diest PJ, van der Wall E: Levels of hypoxia-inducible factor-1 alpha during breast carcinogenesis. J Natl Cancer Inst 2001, 93:309–314
49. van Diest PJ, Vleugel MM, van der Wall E: Expression of HIF-1alpha in human tumours. J Clin Pathol 2005, 58:335–336
50. Maxwell PH, Dachs GU, Gleadle JM, Nicholls LG, Harris AL, Stratford IJ, Hankinson O, Pugh CW, Ratcliffe PJ: Hypoxia-inducible factor-1 modulates gene expression in solid tumors and influences both angiogenesis and tumor growth. Proc Natl Acad Sci USA 1997, 94:8104–8109
51. Stroka DM, Burkhardt T, Desbaillets I, Wenger RH, Neil DA, Bauer C, Gassmann M, Candinas D: HIF-1 is expressed in normoxic tissue and

displays an organ-specific regulation under systemic hypoxia. FASEB J 2001, 15:2445–2453
52. Bauer M, Zhang JX, Bauer I, Clemens MG: ET-1 induced alterations of hepatic microcirculation: sinusoidal and extrasinusoidal sites of action. Am J Physiol 1994, 267:G143–G149
53. Goto M, Takei Y, Kawano S, Nagano K, Tsuji S, Masuda E, Nishimura Y, Okumura S, Kashiwagi T, Fusamoto H: Endothelin-1 is involved in the pathogenesis of ischemia/reperfusion liver injury by hepatic microcirculatory disturbances. Hepatology 1994, 19:675–681
54. Marzi I, Takei Y, Rucker M, Kawano S, Fusamoto H, Walcher F, Kamada T: Endothelin-1 is involved in hepatic sinusoidal vasoconstriction after ischemia and reperfusion. Transpl Int 1994, 7(Suppl 1):S503–S506
55. Grant K, Loizidou M, Taylor I: Endothelin-1: a multifunctional molecule in cancer. Br J Cancer 2003, 88:163–166
56. Nelson J, Bagnato A, Battistini B, Nisen P: The endothelin axis: emerging role in cancer. Nat Rev Cancer 2003, 3:110–116
57. Spinella F, Rosano L, Di Castro V, Natali PG, Bagnato A: Endothelin-1 induces vascular endothelial growth factor by increasing hypoxia-inducible factor-1alpha in ovarian carcinoma cells. J Biol Chem 2002, 277:27850–27855
58. Balkwill F, Mantovani A: Inflammation and cancer: back to Virchow? Lancet 2001, 357:539–545
59. Lewis CE, Pollard JW: Distinct role of macrophages in different tumor microenvironments. Cancer Res 2006, 66:605–612
60. Lin EY, Pollard JW: Role of infiltrated leucocytes in tumour growth and spread. Br J Cancer 2004, 90:2053–2058
61. Ohno S, Suzuki N, Ohno Y, Inagawa H, Soma G, Inoue M: Tumor-associated macrophages: foe or accomplice of tumors? Anticancer Res 2003, 23:4395–4409
62. Tazawa H, Okada F, Kobayashi T, Tada M, Mori Y, Une Y, Sendo F, Kobayashi M, Hosokawa M: Infiltration of neutrophils is required for acquisition of metastatic phenotype of benign murine fibrosarcoma cells: implication of inflammation-associated carcinogenesis and tumor progression. Am J Pathol 2003, 163:2221–2232
63. Lewis C, Murdoch C: Macrophage responses to hypoxia: implications for tumor progression and anti-cancer therapies. Am J Pathol 2005, 167:627–635
64. Jaeschke H, Smith CW: Mechanisms of neutrophil-induced parenchymal cell injury. J Leukoc Biol 1997, 61:647–653
65. Chaudry IH: Cellular alterations in shock and ischemia and their correction. Physiologist 1985, 28:109–118
66. Lehnert M, Arteel GE, Smutney OM, Conzelmann LO, Zhong Z, Thurman RG, Lemasters JJ: Dependence of liver injury after hemorrhage/resuscitation in mice on NADPH oxidase-derived superoxide. Shock 2003, 19:345–351
67. Höckel M, Dornhofer N: The hydra phenomenon of cancer: why tumors recur locally after microscopically complete resection. Cancer Res 2005, 65:2997–3002
68. Hofer SO, Molema G, Hermens RA, Wanebo HJ, Reichner JS, Hoekstra HJ: The effect of surgical wounding on tumour development. Eur J Surg Oncol 1999, 25:231–243
69. van der Bilt JD, Borel Rinkes IHM: Surgery and angiogenesis. Biochim Biophys Acta 2004, 1654:95–104
70. Clemens MG, Bauer M, Pannen BH, Bauer I, Zhang JX: Remodeling of hepatic microvascular responsiveness after ischemia/reperfusion. Shock 1997, 8:80–85
71. Peralta C, Rull R, Rimola A, Deulofeu R, Rosello-Catafau J, Gelpi E, Rodes J: Endogenous nitric oxide and exogenous nitric oxide supplementation in hepatic ischemia-reperfusion injury in the rat. Transplantation 2001, 71:529–536
72. Kuro T, Kohnou K, Kobayashi Y, Takaoka M, Opgenorth TJ, Wessale JL, Matsumura Y: Selective antagonism of the ETA receptor, but not the ETB receptor, is protective against ischemic acute renal failure in rats. Jpn J Pharmacol 2000, 82:307–316
73. Yamamoto S, Matsumoto N, Kanazawa M, Fujita M, Takaoka M, Gariepy CE, Yanagisawa M, Matsumura Y: Different contributions of endothelin-A and endothelin-B receptors in postischemic cardiac dysfunction and norepinephrine overflow in rat hearts. Circulation 2005, 111:302–309
74. Lo AC, Chen AY, Hung VK, Yaw LP, Fung MK, Ho MC, Tsang MC, Chung SS, Chung SK: Endothelin-1 overexpression leads to further water accumulation and brain edema after middle cerebral artery occlusion via aquaporin 4 expression in astrocytic end-feet. J Cereb Blood Flow Metab 2005, 25:998–1011
75. Melillo G: HIF-1: a target for cancer, ischemia and inflammation—too good to be true? Cell Cycle 2004, 3:154–155
76. Semenza GL: Development of novel therapeutic strategies that target HIF-1. Expert Opin Ther Targets 2006, 10:267–280